*Archaeometry* **40**, 2 (1998), 261–279. Printed in Great Britain

# MECHANICAL PERFORMANCE OF QUARTZ-TEMPERED CERAMICS: PART I, STRENGTH AND TOUGHNESS*

V. KILIKOGLOU,[1] G. VEKINIS,[2] Y. MANIATIS[1] and P. M. DAY[3]

[1]*Laboratory of Archaeometry,* [2]*Advanced Ceramics Laboratory, Institute of Materials Science, NCSR Demokritos, Aghia Paraskevi, 15310 Attiki, Greece*

[3]*Department of Archaeology and Prehistory, University of Sheffield, Northgate House, West Street, Sheffield, S1 4ET, UK*

*The effect of quartz temper on the physical and mechanical properties of clay ceramics and the elucidation of the underlying mechanisms that are responsible for these effects are presented here. Characteristics studied included bulk density, open and closed porosity, density of impervious portion and fracture morphology. Mechanical behaviour was studied by measuring energy dissipation during fracture, Young's modulus, initial fracture toughness and strength in flexure. The significant increase in toughness with quartz volume fraction is explained by the development of a model that accounts for the crack distribution around the grains. The archaeological implications of the work are discussed on the basis of all the parameters that might affect the potter's choices of raw materials.*

*KEYWORDS*: CERAMICS, QUARTZ, ELASTICITY, MECHANICAL PROPERTIES, POROSITY, STRENGTH, TEMPERING, TOUGHNESS

## INTRODUCTION

One of the major drawbacks of ceramics is their brittleness. Even high-strength pottery may fail catastrophically if a large flaw is present in the material. This problem has often been addressed by introducing an amount of non-plastic material—temper—into the clay paste. Intentional tempering was known and practised in antiquity and has appeared, at least in the prehistoric Aegean, in a variety of forms: (a) the addition of crushed or naturally weathered non-plastics (calcite, quartz, etc.), (b) the mixing of a fine, plastic clay with another, relatively poor in clay minerals, and (c) the use of a single clay containing naturally occurring non-plastics.

The reasons that potters tempered or mixed their clays are many and varied. Technological studies of archaeological ceramics generally have concentrated on the effects of two influences in such choices: that of the environment (e.g., the availability of raw materials) via the concept of ceramic ecology (Matson 1965; Kolb 1989), and the functional/optimizing approach which has sought to justify potters' actions through the observation of the suitability of pottery materials for their intended use. But, equally, such choices can be influenced strongly by cultural considerations (Day 1988 and forthcoming). Without a full contextual study, it is difficult to suggest with certainty which of the above reasons dominated the choice and treatment of raw materials in individual cases. However, many clay paste recipes, which became part of a strong tradition, at least had their roots in functionally specialized ways of tempering and mixing clay bodies.

We do know, however, that, irrespective of whether recipes are 'ideal' or not, tempering influences a number of performance characteristics of clays and ceramics. It increases clay

*Received 12 May 1997, accepted 22 October 1997.

workability, reduces shrinkage, assists in even drying and promotes some mechanical properties at the expense of some others (Rice 1986; Rye 1976).

The most common rock tempering materials can be classified in two groups: calcite-based materials that chemically react with the clay minerals during firing and materials that are essentially inert at the usual firing temperatures (quartz, feldspar, etc.). The effects of temper on the performance, including mechanical performance, of ceramics was first studied and discussed in the pioneering work of Shepard (1965). Since then several studies have been reported in the literature. Much attention has been given to the explanation of the beneficial effects of certain tempering materials used in the prehistoric New World, with particular reference to crushed shell in comparison to sand. The main shell-tempered pottery characteristics studied have been thermal shock resistance (Steponaitis 1984; Bronitsky and Hamer 1986), strength (Bronitsky and Hamer 1986; Feathers 1989) and toughness (Feathers and Scott 1989). It has been demonstrated generally, through simulation tests, that shell can produce stronger and tougher ceramics than sand, which was replaced as a temper during the Late Woodland period in eastern North America. The same applies to limestone, although it was not used systematically, compared to grit or grog (Hoard *et al.* 1995). Besides enhanced mechanical properties, there are further benefits in the use of calcite-based tempers, summarized by Hoard *et al.* (1995): increase of workability, similar thermal expansivity to clay and a plate-like structure that aids crack propagation arrest, in a similar way to modern fibre-reinforced ceramics. However, calcite can be problematic at high firing temperatures (Maniatis and Tite 1981; Rice 1986) and, therefore, it can only be used as temper at low-firing temperatures, less than *c.* 700 °C, where ceramic bodies remain essentially unvitrified and the maximum strength they develop is, thus, close only to their green strength.

On the other hand, there have been many cases of high-fired *and* quartz-based-tempered pottery. A typical example is that of Punic amphorae transported as containers whose specifications probably required high strength to withstand large loads during transportation. It has been established that they were fired at temperatures ranging from 800 to 1080 °C (Maniatis *et al.* 1984). A similar case is that of the Early Minoan storage jars from the Mirabello area in eastern Crete, possibly used for liquids. These are large vessels (≈30 l), with thin walls (≈3 mm thick) to reduce weight, that were fired at 1000–1080 °C to create strong bodies (Whitelaw *et al.* 1997). In both examples quartz-based tempers were used by the ancient potters, either in the form of sand or of earth rich in quartz.

The central aim of the present study is the clarification of the effect of quartz temper on the physical and mechanical properties of clay ceramics and the elucidation of the underlying mechanisms that are responsible for these effects. Test specimens containing variable amounts (0, 5, 10, 20, 40% vol) of quartz, with a range of grain sizes (average diameter 750, 450, 250, 150 $\mu$m), were prepared for this purpose. Specimen characterization included bulk density, open and closed porosity, density of impervious portion (a measure of sintering extent) and fracture morphology. Mechanical behaviour was studied by measuring the following properties which provide complementary information: energy dissipation during fracture $G$ (the work of fracture), Young's modulus $E$, initial fracture toughness $K_{ic}$ and strength in flexure (transverse rupture strength, TRS). Additionally, in Part II of this work (Vekinis and Kilikoglou 1998, this volume), the Hertzian point loading strength $\sigma_H$ and abrasive wear resistance $Q$ were also measured and proposed as alternative tests, easily applicable to archaeological pottery.

The methodology that has usually been followed in studies of the mechanical properties of

archaeological pottery is to test replicates of ancient ceramics (Feathers 1989), imitating their method of manufacture but restricting the temper compositions only to the levels contained in the pottery under study. While, by this approach, a straightforward comparison among some realistic case studies may be achieved, there are methodological problems. As will be shown in this work, relatively small differences in temper concentration may have a significant impact on the mechanical performance and, therefore, a systematic study is always necessary (i.e., using a range of temper concentrations and grain sizes), in order to avoid the loss of important information.

The main reason that mechanical tests are performed on replicates rather than ancient ceramics is that most of these tests require multiple specimens—in order to ensure the statistical significance of the results—of specific geometry and large size that cannot easily be obtained from sherds, especially when the latter exhibit curvature (Feathers 1989). In addition, they might have been degraded through use and burial conditions.

## EXPERIMENTAL

### *Materials and processing*

Test specimens were manufactured using a calcareous clay from the area of Pikermi in Attica, Greece, a clay which is normally used by the brick industry. Its chemical composition appears in Table 1. Such calcareous clays are known to display excellent post-firing mechanical properties, due to the homogeneous cellular microstructure they develop in the firing temperature range 850–1050 °C (Maniatis and Tite 1981). The clay was gently crushed, sieved though a 250 mesh cloth and then a fraction with grain size $< 30\,\mu m$ was obtained by levigation. This fraction was used as the matrix material for all specimens. It was mixed with naturally weathered sand (99.5% $SiO_2$) of four different average grain sizes D = 750 $\mu$m, 400 $\mu$m, 250 $\mu$m and 100 $\mu$m in volume fractions of $V_f$ = 0%, 5%, 10%, 20% and 40% for each grain size. The 750 $\mu$m-40% combination was not included because the fired briquettes were too weak to test accurately. In

Table 1 *Chemical composition by X-ray fluorescence of the base clay*

| *Element* | *Concentration (%)* |
|---|---|
| $Al_2O_3$ | 19.2 |
| $P_2O_5$ | 0.2 |
| $K_2O$ | 2.6 |
| CaO | 9.5 |
| $SiO_2$ | 41.7 |
| $TiO_2$ | 0.9 |
| MnO | 0.1 |
| $Fe_2O_3$ | 8.6 |
| MgO | 1.9 |
| $Na_2O$ | 0.3 |
| Loss on ignition | 14.3 |
| Total | 99.3 |

this way, a total of 16 different powder mixes with all combinations of variables were prepared. Water was added to the mixes to provide plasticity and briquettes of size 100 × 60 × 10 mm were produced by manual uniaxial compaction. They were then completely covered by plates made of plaster of Paris, to ensure homogeneous drying, and left for over five days at ambient temperature and humidity. Firing took place in air at 950 °C with a heating rate of 200 °C/h and a soaking time of one hour. Some untempered briquettes were also fired at 800 °C and 1100 °C using the same schedule. These three firing temperatures were chosen because they create different microstructures: at 800 °C there is no vitrification present in the microstructure, at 950 °C there is a high concentration of thin glass-like filaments (extensive vitrification), while at 1100 °C there is a higher concentration of thick filaments (total vitrification). After firing, the larger surfaces of the briquettes were ground parallel on a number 1200 carborundum wheel and cut by a diamond wheel to produce rectangular test bar specimens of approximate size 10 × 10 × 60 mm.

*Characterization and testing*

*Porosity and density determination* The bulk density (dry weight/exterior volume, g/cm$^3$), density of impervious portion (dry weight/volume of impervious portion, g/cm$^3$) and the open porosity were determined according to ASTM C20-92 (ASTM 1993).

The theoretical density, $\rho_{th}$, of the materials was calculated taking the density of the base fired clay, found to be $\rho_c = 2.7$ g/cm$^3$, that of quartz as $\rho_q = 2.75$ g/cm$^3$ and using the standard rule of mixtures equation (Ashby 1993).

*Young's modulus* Young's modulus was determined both in bending and in compression (for accuracy) by measuring the gradient of the linear part of the load-deflection curve just before fracture initiation. The compliance of the loading system (machine and jigs) was determined by calibration using a precision ground steel specimen, of the same size as the experimental specimens. $E$ in bending was determined from the curves of the bending tests, using elastic beam theory (Vekinis *et al.* 1993), as

$$E_{bend} = \frac{dP}{dx}\frac{\Delta s^3}{4bd^3} \tag{1}$$

where $\Delta s = S_2 - S_1$ (Fig. 1) and $P$ is the load.

For the compression tests, rectangular, parallel-sided ceramic and steel (for calibration)

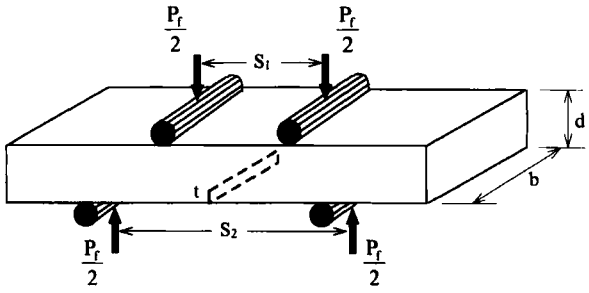


Figure 1 *Specimen characteristics and loading configuration for the four-point bend test.*

specimens, of approximate size 10 × 10 × 20 mm, were prepared. All specimens were subjected to uniaxial compression at a loading rate of 100 μm/min. To avoid misalignment problems, the ends of the specimens were ground parallel with number 1200 SiC and, in order to avoid chipping and spalling of the specimens, copper foil was placed between the surface and the anvils in all tests. For confirmation, a small number of specimens were also tested by ultra-sonic equipment with comparable results.

*Fracture energy (toughness)* In the case of homogeneous, truly brittle materials, exhibiting unstable crack propagation (Fig. 2 (a)), the fracture energy can be determined by the toughness $G_{Ic}$ (see 'Appendix'). According to equations (4) and (5), its determination requires independent measurement of $K_{Ic}$ and Young's modulus $E$. $K_{Ic}$ was, therefore, measured in four-point bending using the straight-edge-notched-beam (SENB) configuration (Fig. 1). In order to ensure accuracy and reproducibility, the surfaces of such specimens need to be parallel with as few surface imperfections and sharp edges as possible. The specimens were prepared as follows: after diamond sectioning from identical fired briquettes, rectangular beam specimens were ground parallel and polished on a number 1200 carborundum polishing wheel. Their edges were slightly rounded to avoid stress concentrations during loading and the notch was diamond machined using a 0.15 mm thick wafering blade on the centre of a surface normal to the original pressing direction. The specimen size (10 × 10 × 60 mm) ensured minimal internal shear stresses during loading while ensuring that a statistically adequate number of quartz grains was included in the eventual fracture surface. The notch depth was kept close to 2 mm (≈20% of height) to avoid edge stress effects during testing.

In all tests the specimens were loaded in a self-aligning bending jig on an INSTRON 1195, 100 kN testing frame at a constant loading rate of 50μm/min. The load as a function of displacement was recorded as shown in Figure 2.

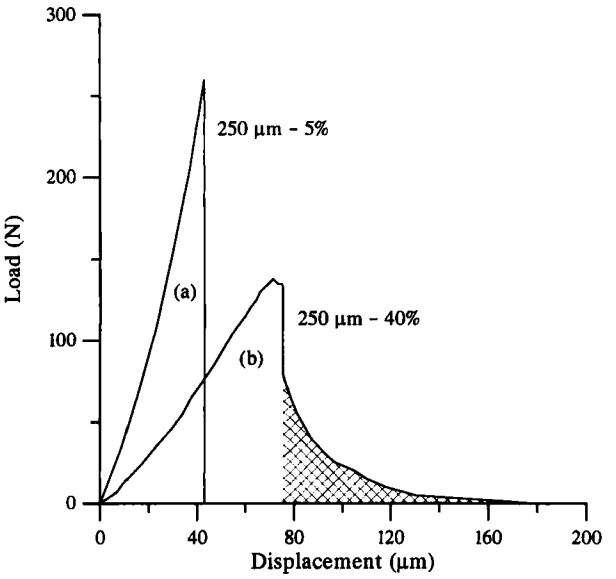


Figure 2 *Typical uncalibrated load-displacement curves for the two types of fracture:* (a) *unstable;* (b) *stable.*

For the specimens that failed in an unstable manner (Fig. 2 (a)), $K_{Ic}$ was determined using the analysis of Srawley (1976):

$$K_{Ic} = \frac{3P_f(S_2 - S_1)}{2bd^2}\sqrt{\pi t}\,F(\alpha) \tag{2}$$

where $P_f$ is the load at fracture (maximum load in the load-displacement curves) and $F(\alpha) = 1.122 - 1.121\alpha + 3.74\alpha^2 + 3.873\alpha^3 - 19.05\alpha^4 + 22.55\alpha^5$ and $\alpha = t/d$. Our measured $K_{Ic}$ values were corrected for finite notch width following the results of Munz *et al.* (1980) dividing by a factor of 1.25. The fracture energy, $G_{Ic}$ in this case, was calculated using equations (4) and (5) (see 'Appendix').

In the cases where specimens exhibited stable crack propagation during fracture (Fig. 2 (b)), the total fracture energy was the sum of $G_{Ic}$ (determined as above) and the toughening component $G_t$ ('Appendix') as obtained by integration of the area under the stable part of the curve. $G_{Ic}$ was determined in the same way as in the specimens that failed unstably. In both cases Young's modulus values for each specimen were required (equation (4)).

*Fracture strength* Similar preparation and configuration (without the notch) was used for the three-point bending transverse rupture strength (TRS, often referred to as modulus of rupture) tests, calculated using the standard TRS equation (Bronitsky 1986). Failure during this test initiates at the tip of the maximum size flaw. Due to the random size and position of the flaws, usually created during manufacture, one expects wide variation in the results and, therefore, multiple tests are usually required from which the Weibul parameters are determined. However, tempering produces an homogeneous distribution of flaws of equal size and, thus, simple averaging of the results was sufficient. In this work at least seven specimens from each grade and volume fraction were tested.

Finally, the micromechanics of fracture were investigated by dynamic *in situ* microscopy (Kilikoglou *et al.* 1995). A high resolution video camera and colour monitor were used to observe and record the fracture process for all specimens at magnifications up to 100 times. This, in conjunction with a fast video printer, provides the possibility of monitoring the progress of fracture and allows correlation with the load-deflection curve in real time. In addition, scanning electron microscopy (SEM) was used to study the fracture surfaces and, in particular, the quartz-matrix interfaces.

## RESULTS AND DISCUSSION

The two main modes of fracture, unstable fracture and stable crack propagation during bending, are illustrated in Figure 2. The figure shows the actual load-deflection curves obtained for specimens containing 5%, curve (a), and 40%, curve (b), quartz of average grain size 250 $\mu$m. It can be seen that in the first case (Fig. 2 (a)) the material exhibits a typical, unstable brittle fracture behaviour with complete fracture at the maximum point. All specimens containing 0, 5 and 10% quartz, of all grain sizes, exhibited similar behaviour, for all quartz sizes. A different picture was displayed by the 20 and 40% materials as illustrated by the example of Figure 2 (b). On failure, the load drops sharply but is arrested and thereafter decreases gradually until complete separation, which defines stable crack propagation. The 20% and 40% materials exhibit remarkable crack stability and a considerable amount of energy (toughening $G_t$ given by the shaded area under the curve) is dissipated until final fracture.

The results indicate that there exist two different regions as far as crack propagation is

concerned. The region of unstable crack propagation for low $V_f$ and the region of stable crack propagation for high $V_f$ materials. The precise volume fraction at which fracture becomes stable could not be established with certainty because the stiffness of the loading machine may in fact influence this. The intrinsic energy $G_{ic}$ and the total energy dissipated for all materials is shown in Figure 3. As there was considerable 'intertwining' of the curves of materials of same $V_f$ but different quartz size, the results are enclosed in an envelope. The total energy measured for the second region (for $V_f > 10\%$) is significantly higher than that for the first region ($V_f < 10\%$). It can be seen that $G_{Ic}$ is approximately constant for all volume fractions and falls in the range 25–35 J/m$^2$. However, the total energy $G$ increases dramatically for the higher $V_f$ materials as it includes the contribution of the energy dissipated during stable fracture $G_t$. Figure 3 also includes the total energy $G$ for non-tempered specimens fired at 800 and 1100 °C for comparison with the other replicate specimens fired at 950 °C. At higher firing temperatures (1100 °C), vitrification is extensive and fracture remains unstable. However, when vitrification is kept at very low levels (e.g., by firing at 800 °C), the material displays significant stable crack propagation with significant energy dissipation.

Similar stable fracture behaviour has been reported for grog-, grit- and limestone-tempered materials fired at only 600 °C (Hoard *et al.* 1995), albeit at very low fracture loads as the materials were effectively in the green state.

The fracture behaviour of the specimens used for the strength measurements (TRS) was very similar to that observed for the fracture energy tests. Materials containing up to 10% of quartz of all grain sizes failed in an unstable manner while those containing 20 and 40% exhibited stable crack propagation. As expected, the TRS, which, as discussed in the 'Appendix', is a measure of the flaw content of the material, decreases significantly as the amount of temper increases. At the

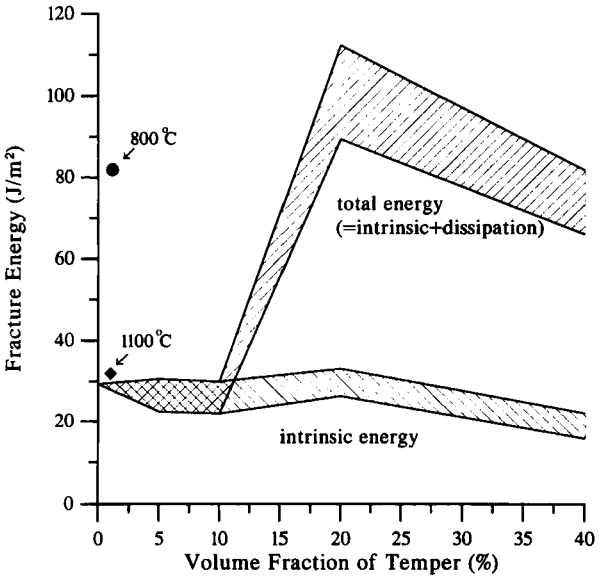


Figure 3 *Fracture energy range as a function of volume fraction* ($V_f$). *For* $V_f \leq 10\%$ *energy dissipation during fracture equals zero. The solid black circle and diamond represent the total energy of of non-tempered specimens fired at 800 °C and 1100 °C respectively.*

same time it is also influenced by quartz grain size, as shown in Figure 4. In the present work all replicates were made in the same way and special care was taken to eliminate extraneous flaws. This is reflected in the standard deviation of TRS values which was found to be only about 10–20% in all cases, showing relative homogeneity within each test series. This indicates also that fracture must have initiated at flaws of similar size which are probably associated with the quartz temper. For $V_f = 5$ and 10%, TRS appears to decrease continuously. On the other hand, for $V_f$ = 20 and 40%, after the initial decrease, which is larger than that of lower $V_f$, TRS values appear to level out for all grain sizes used, indicating that the effect of grain size on TRS becomes less important when the concentration of quartz is over about 20%. This is important and its origin is discussed in detail below (damaged zone). Finally, untempered specimens fired at 1100 °C displayed similar strength to those fired at 950 °C, whereas the strength of the materials fired at 800 °C was only about half that. This is shown in Figure 5 where both the toughness and strength results for the untempered materials are plotted against firing temperature. The values of strength and fracture energy at 850 °C were not actually measured but were inferred by the fact that in calcareous clays extensive vitrification is developed at this temperature and remains constant up to 1050 °C (Maniatis and Tite 1981). It can be seen that, as the strength increases with temperature, the toughness decreases. At temperatures greater than about 850–900 °C both quantities reach 'steady-state' values. It is clear that, apart from any other considerations, the presence of vitrification (below or above a firing temperature of about 800–900 °C) significantly affects the mechanical behaviour of the materials.

Additional evidence for the existence of two fracture regimes (low $V_f$–high $V_f$) was displayed by the porosity results. Figure 6 shows that the apparent (open) porosity at 950 °C is approximately stable for $V_f$ = 0–10% but increases significantly for higher volume fractions. The apparent porosity concerns the clay matrix and any voids between inclusion-clay interfaces, as quartz has practically no porosity at all. In the present case the clay matrix is highly calcareous

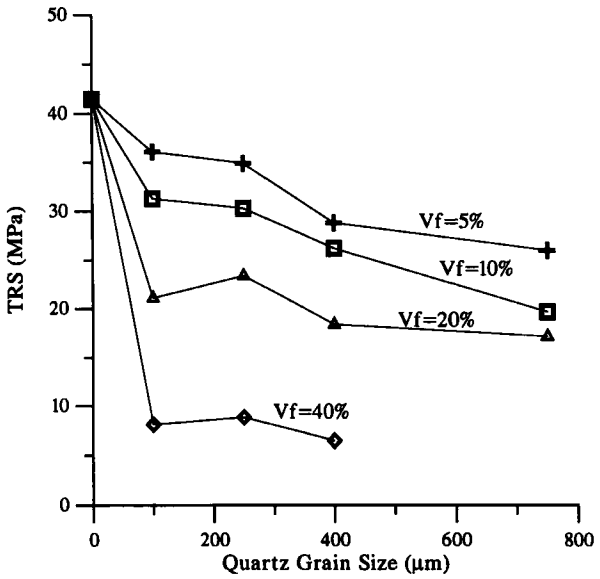


Figure 4 *Transverse rupture strength as a function of quartz grain size and volume fraction.*

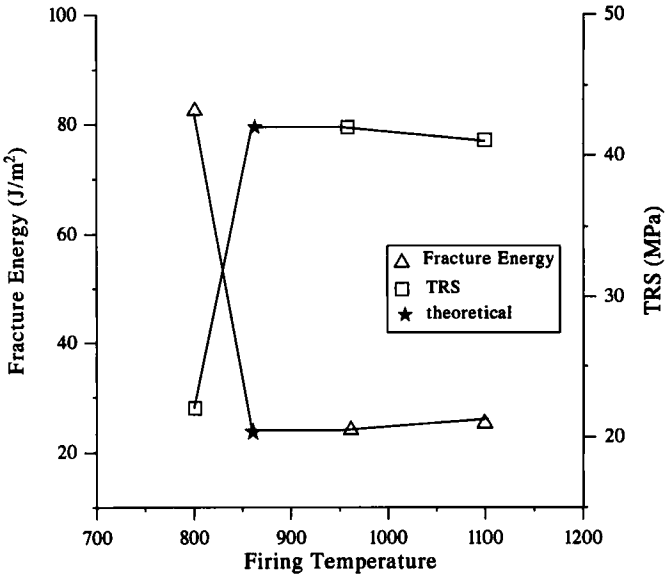


Figure 5 *Transverse rupture strength and fracture energy of untempered specimens as a function of firing temperature.*

and for this reason is very porous after firing (Tite and Maniatis 1975). Matrix porosity is basically created by release of gases (mainly $CO_2$) or evaporation of water during firing as well as any cracks that may develop during drying and firing. For specimens with $V_f = 20$ and 40%, additional porosity appears to arise as a result of some other mechanism which acts in parallel to

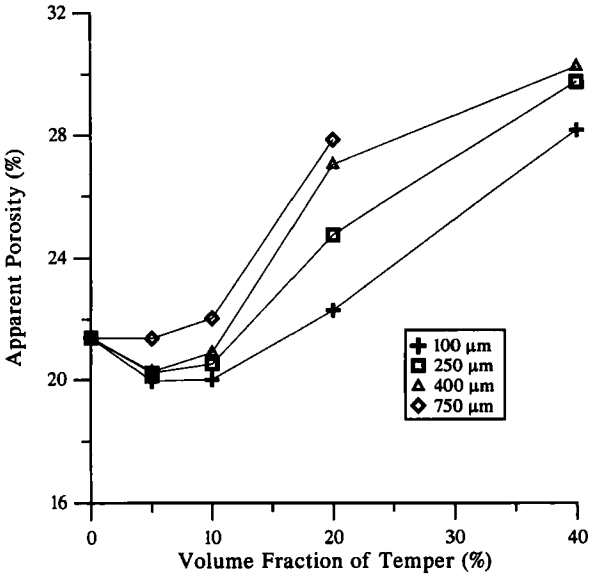


Figure 6 *Apparent porosity as a function of quartz volume fraction and grain size.*

the normal one. A similar picture is displayed by the closed porosity (given by the difference between the density of the impervious portion and the theoretical density) shown in Figure 7. The theoretical density in each case was calculated using the rule of mixtures. We see that, for the case of 40% quartz, for all the grain sizes the density of the impervious portion reaches the theoretical value, which means that there are almost no closed pores in the material.

Extensive scanning electron microscope observations of the microstructure indicate that, for $V_f$ above a 'threshold' of 10–20%, the materials contain an unusually large amount of microcracks. This we believe to be the result of quartz-matrix interaction and can explain the observed mechanical behaviour of the materials. The effect of quartz on the porosity can be understood by considering what happens to the clay-quartz system during drying and firing. During drying, water surrounding the clay platelets evaporates and the platelets draw closer together, causing shrinkage which results in hydrostatic compressive stresses on the quartz inclusions (Rice 1986). As a result, tensile stresses develop on the matrix material around them. SEM observations showed that, in the specimens containing quartz, microcracking was evident in the immediate vicinity of the quartz inclusions. This microdamaged area around each quartz grain can be defined as the 'damaged zone' of radius $r_{\text{eff}}$ which is much larger than the actual radius of the quartz grain. Upon firing, this damaged zone is further extended due to the loss of crystalline water and further matrix shrinkage which results in an extensive matrix-inclusion debonding (Kilikoglou *et al.* 1995). As we will show later, the actual extent of this damaged zone determines the strength and toughness of the material. Additional support for the above was given by the bulk density measurements. It can be seen in Figure 8 that bulk density (as per cent of theoretical) displays a continuous decrease with increasing $V_f$. An increased amount of quartz results in increasing volume of pores and, therefore, a decrease in matrix bulk density.

The matrix-inclusion debonding is supported by the Young's modulus results. Even though quartz has a higher modulus (80 GPa) than fired clay (22 GPa) and, thus, the modulus of the fired

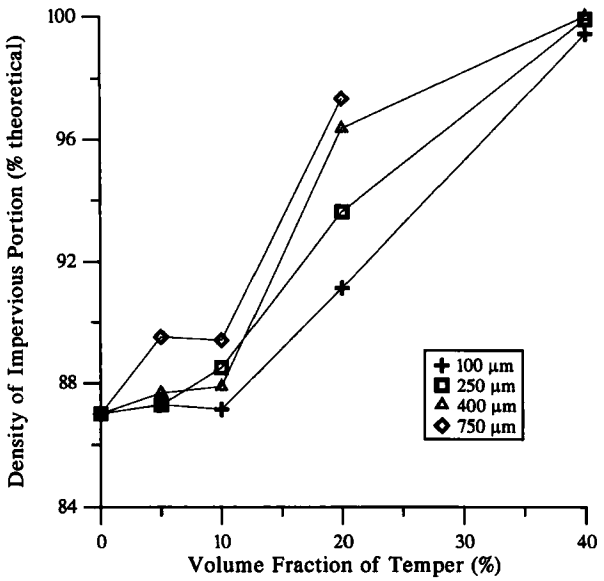


Figure 7 *Density of impervious portion as a function of quartz volume fraction and grain size.*

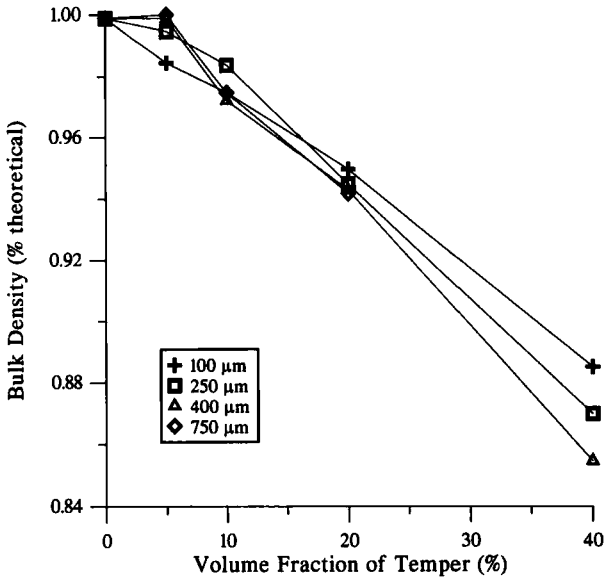


Figure 8 *Bulk density decrease (expressed as % theoretical) as a function of quartz volume fraction and grain size.*

composites should increase with increasing $V_f$, the opposite was observed (Table 2). $E$ decreases significantly with increasing $V_f$ (by a factor of about three for $V_f$ = 40%) and this decrease appeared to be almost independent of the grain size. Due to the existence of quartz-matrix debonding, we can approximately model the tempered materials as clay containing a population of closed pores of fixed size, using the result of MacKenzie (1950):

$$E = E_0(1 - 1.9V_f + 0.9V_f^2) \tag{3a}$$

where $E_0$ is the modulus of the untempered ceramic and $V_f$ the volume fraction of pores. For illustration, in our case untempered ceramic has $E_0$ = 22.4 GPa and for $V_f$ = 40%, equation (3a) gives $E_{40\%}$ = 8.6 GPa, which falls within the range of the experimental results. Therefore, it can be suggested that the material behaves like one containing an equivalent population of pores of effective diameter equal to that of the quartz inclusions. The debonding between the grains and

Table 2 *Experimental (in bending) and theoretical Young's modulus* (E) *values. The experimental values of Young's modulus for each* $V_f$ *are shown as the mean of all quartz grain sizes. For the theoretical calculations, the measured Young's modulus of the base clay (22.4 GPa) was used*

| *Volume fraction of temper* $V_f$ *(%)* | *Experimental* E *(GPa)* | *MacKenzie* E *(GPa)* | *MacKenzie + Wang (GPa)* |
|---|---|---|---|
| 0 | 22.4 | 22.4 | 22.4 |
| 5 | 19.7 | 20.3 | 20.5 |
| 10 | 18.0 | 18.3 | 18.5 |
| 20 | 12.3 | 14.7 | 13.6 |
| 40 | 6.9 | 8.6 | 7.2 |

the matrix is magnified by the quartz inversion accompanied by expansion that takes place at 573 °C, in conjunction with matrix shrinkage at temperatures >800 °C and its differential contraction during cooling. The contribution of the damaged zone results in a further decrease in $E$ and can be modelled using the results of Wang (1984) which takes into account the microcracking around the pores and in the damaged zone:

$$E = E_0[\exp -(1.46V_f + 9.82V_f^2)] \tag{3b}$$

This contribution amounts to only an additional 10% reduction in $E$ which actually at high $V_f$'s brings the theoretical values closer to the experimental (Table 2). This small reduction is reasonable as microcracks are fine and their closure results in very limited deformation.

The effective damaged zone radius $r_{eff}$ is given by the distance from the centre of the inclusion (of radius $r_0$) over which the local stress is continuously decreasing until it becomes equal to the green strength, $\sigma_g$, of the matrix where matrix damage is negligible. A graphic representation of the effective damaged zone is given in Figure 9. The area of a damaged zone multiplied by the number of inclusions intersecting the fractured surface defines the damaged area $A_{eff}$. It has been shown (Kilikoglou *et al.* 1995) that for $V_f$ up to 10% the damaged area is a fraction of the fractured surface, while at higher $V_f$ levels the individual 'damaged zones' interact with each other and produce extensive microcrack networks that cover the whole specimen. During fracture, it is this microcrack network that encourages crack deflection and bifurcation thus increasing the energy dissipation.

Mechanisms of fracture were observed by *in situ* optical microscopy and scanning electron microscopy. The main crack propagates during loading by matrix cracking or along a debonded interface. In the case of untempered specimens, the crack was observed to propagate approximately straight, but at large $V_f$ it was observed to weave appreciably from one inclusion to another, resulting in energy dissipation by the mechanisms of deflection (Fig. 10) and bifurcation (Kilikoglou *et al.* 1995, fig. 8). The energy dissipated by these mechanisms is

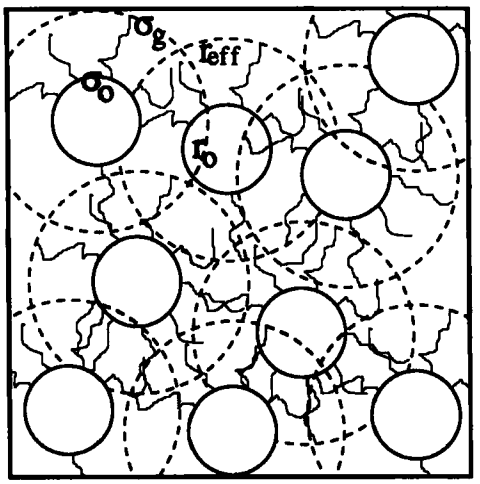


Figure 9 *Graphical representation of the damaged zones (dashed circles) surrounding the quartz grains (grey circles) in a fracture surface.* $r_0$ *= radius of quartz grain;* $r_{eff}$ *= radius of damaged zone;* $\sigma_0$ *= quartz-clay interface stress;* $\sigma_g$ *= green strength of clay body.*

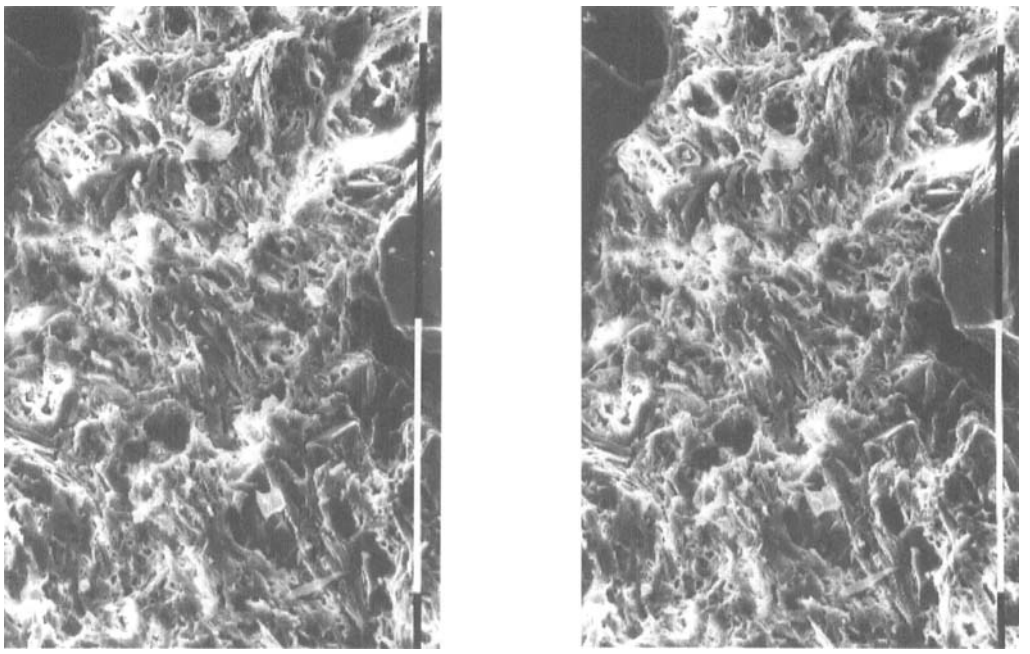

Figure 10 *Pair of stereoscopic SEM microphotographs showing a characteristic fractured surface after a four-point bending experiment (specimen with* $V_f$ *= 20% and* D *= 450 μm). The surface displays a step-like nature which is the result of a zigzag crack propagation, absorbing significant amounts of energy. Photographs were taken at a relative angle of 8°, each section of bar = 100 μm. The effect can be better observed using a stereoscopic viewer.*

probably further increased by friction during pull-out of the quartz grains from the matrix during cracking, as observed during the *in situ* fracture experiments (Kilikoglou *et al.* 1995). This mechanism has also been observed in other types of ceramic materials (Vekinis *et al.* 1990). The damaged zone model is supported by the results of the open and closed porosity. Because of the completely microcracked matrix, there is practically no closed porosity as the extensive network at high $V_f$ ensures that all pores and microcracks connect with the surface.

In general, the results of this work show that there is an optimum concentration of temper for ceramics (around 20% for vitrified calcareous matrix in this case) at which the materials increase their toughness with a reduction of strength of about 50%. Further increase in temper reduces strength to dangerously low levels without any increase in toughness. The exact threshold of nonplastic volume fraction at which toughness increases considerably varies and depends on clay type, nonplastic composition and firing temperature. However, in any case this increase in toughness (producing crack stability) can be very beneficial in pottery performance during use or transport as can be concluded from the present results, which can be applied to archaeological pottery of similar clay type and temper composition in order to predict its behaviour.

## CONCLUSIONS OF EXPERIMENTAL WORK

The mechanical behaviour of the quartz-calcareous clay system is very sensitive to the proportion of quartz inclusions. At low volume fraction of inclusions (less than about 10%)

the system behaves as a normal brittle ceramic, but at higher quartz contents the material displays significant energy dissipation (toughening) during fracture.

The toughening enhancement appears to be the result of the formation of an extensive network of microdamage during drying and firing which increases energy dissipation via crack wandering. However, this results in a substantial reduction of the strength which can be controlled by keeping the amount of temper in the area of 20%.

The toughening enhances crack propagation stability and there is evidence that it may have been known about in the past, as it provides a means of ensuring that any cracks in vessels and pots would not propagate catastrophically but would provide some warning and allow for repairs.

## EPILOGUE: ARCHAEOLOGICAL IMPLICATIONS OF THE RESEARCH

The results presented here elucidate the beneficial effects of non-plastic material in prepared clay bodies, and clarify the proportions of temper which are optimal in the complex interplay between the properties of strength and toughness. The questions arise as to how such data should be used with archaeological material, whether there can be a clear, predictive role for these observations, and in what way engineering and design analysis interface with past human behaviour.

There are a number of ways in which the toughness of a pot may relate to its function. It might be suggested that a vessel's portability has a close link to a need to withstand mechanical shock. Vessels used in bulk transportation are obvious cases in point. For example, amphorae transported as containers in maritime trade would need to withstand both shocks during movement and pressure from being stacked together. A characteristic example are the water jars. They are specifically made with high porosity to keep the water cool and, therefore, exhibit high toughness. At the same time they have to carry some strength in order to cope both with the weight of their contents and persistent movement involved in filling them and pouring out their contents. Yet it is not only these portable vessels which make special demands on their ceramic matrices. For instance, the large storage jars of the prehistoric Aegean, up to 2 m in height, must not have been moved regularly. Yet the thickness of their walls makes them very reliant on even drying during the vessel's building, which may be one factor which leads to the coarse nature of their fabric. Equally these vessels were transported to the locations of their use, most likely by pack animal, and, thus, need to withstand such stresses of transportation. In contrast, highly decorated small cups, bowls and jugs are often made of much finer clays, a quality which may relate both to their weight as well as to their less arduous usage.

A more obvious example of functionally demanding pottery are cooking vessels, which, in addition to having to withstand mechanical shock, also have to cope with regular heating and cooling. The ability to withstand such thermal shock, although forming a separate problem in examining the performance of ceramic materials, is, nevertheless, linked to qualities of toughness and the need to avoid catastrophic failure of the vessel.

If, in such highly differentiated assemblages, we observe varied demands made of different vessels and that these vessel categories are correlated with very different ceramic materials, then, perhaps, it may be possible to use the observations of research on mechanical properties in a *predictive* fashion. For instance, this might be achieved by taking an assemblage whose morphological variation does not provide detailed information on usage and predicting the general function of vessels, by the nature and quantity of their non-plastic inclusions.

Yet there are many problems which stand in the way of such a correlation of composition to function. Firstly, function itself may vary between that intended by the potter and the actual function of the pottery in use (Skibo 1992); secondly, this correlation assumes that potters choose and manipulate raw materials in a somewhat optimizing fashion. In reality the factors affecting potters' choice are many and varied and to impose our view of efficiency and performance on the past is difficult. There are circumstances where our predictions work, but others where they seem to fall short of being a whole explanation of the nature of a ceramic fabric. It is valuable to consider why this is so in view of the role that studies of mechanical performance can play in archaeological ceramics.

The literature on this subject revolves around some key concepts: decision making, optimization and evolutionary theory. Diachronic change in the nature and proportion of temper used in pottery has been explained by a retrospective, best-fit justification for the changes in materials observed. This is an example of where research on mechanical performance can set such changes in a different light. Simply being able to demonstrate some of the changes from 'suitable' ceramic pastes to 'less optimal' materials over time prompts us to question some aspects of a Darwinian evolutionary perspective (O'Brien *et al.* 1994). On behalf of the latter, it has been argued that 'changes in technology are driven by selection for *performance characteristics*, which in turn are driven by changes in the various behaviours of the makers and users of the materials as they respond to the selective environment' (O'Brien *et al.* 1994, 261). Yet this is to underestimate the myriad factors which affect the materials and design of a given vessel. Of course, it seems clear that pots which are so 'sub-optimal' that they fail consistently will not continue to be produced; yet, that potters frequently use materials which they know to be unsuitable, is also clear (Day forthcoming).

Such a situation occurs because pots and their manufacture are not affected by economic thinking only. Not only do the objects produced often play important social roles within a society, but also the processes involved in their creation frequently have their own important social life. What is chosen as a raw material and how it is transformed comprises a set of technological practices which frequently transcend what might appear to us matters of practicality or suitability. It has been demonstrated how partial perception (van der Leeuw 1989) and social agency (Dobres and Hoffman 1994) show the craftsperson as an active individual reflecting and affecting their social circumstances, through their choices and actions (e.g., Lemonnier 1993). In effect, the technological practice forms part of an active creation of social identity and position.

The routines of craft practice frequently form technological *styles* which, regardless of technical demands, take on their own importance in terms of a craft group's identity (Wright 1986; Day forthcoming). Thus, the way in which materials are chosen and manipulated may be a good indicator of social groupings or the transmission of knowledge. In this way, just as the environment can be viewed as a stage on which potters act to create their product (Matson 1965), so can technical requirements and social identity be seen as influential on the resulting ceramic paste. It is clear, then, that many of these factors may have very little to do with function/optimality.

It is for these reasons that the approach to change in the design and technology of ceramics has been problematic. In its emphasis on selectivity it has given precedence to adaptation, but does not deal well with historical *discontinuity* of the sort that is observed, for example, in the prehistory of both Britain and the Aegean. Fabrics such as those dominated by grog and calcite tempering in the Late Neolithic and Early Bronze Age of Crete and the Cyclades have their

background in the technological practice of different human groups. They can, potentially, be used to identify groups of pottery over broad geographical areas whose technological traditions are related (Whitelaw *et al.* 1997) or perhaps even to indicate the movement of people.

From this, it is suggested that there is a range of elements whose study may lead to an understanding of pottery and that it is as important to see *differences* between pottery groups themselves, and between the pottery and a theoretical 'ideal' that we might construct from intended ceramic function and ceramic ecological resources. As variance from an optimum is potentially of great interest, it is necessary to conduct work such as that presented here on mechanical properties in order to provide a baseline by which to assess observed variation (potential decisions which are not taken). By doing this we perceive more clearly examples where factors *other* than performance took precedence in the potters' and consumers' minds.

There are additional ways in which studies of ceramic mechanical properties can have important implications for archaeology. Firstly, that there *are* cases of clear diachronic change, either short- or long-term, which herald improved performance—aspects which can add to our knowledge of major innovations and, ultimately, to the forming of a history of technology. Secondly, the technological and, especially, the clay preparation traditions that have been outlined above generally involve fabrics which are specialized for one type of pot. Over time they may be used for the manufacture of vessel types for which the clay mix was not designed originally. We would take this latter consideration to indicate a clay mix which has taken on a meaning beyond the purely functional.

Overall, the improved understanding of ceramic performance criteria will aid appreciation of the complex factors behind the choices potters took. Much has been made of the changes in ceramic fabrics in the American Midwest, yet the insistence on interpreting those data in terms of optimization detracts from the potential wealth of social and other information to be gained in that area and certainly from more complex assemblages elsewhere, notably in the Mediterranean and Near East.

## ACKNOWLEDGEMENTS

We would like to thank M. A. Cau Ontiveros for the X-ray fluorescence analysis of the clay from Pikermi.

## REFERENCES

Ashby, M. F., 1992, *Materials selection in mechanical design*, Pergamon Press, Oxford.

Ashby, M. F., 1993, Criteria for selecting the components of composites, *Acta Metallurgica et Materialia*, **41** (5), 1313–35.

Ashby, M. F., and Jones, D. R. H., 1996, *Engineering materials I*, 2 edn., Pergamon Press, Oxford.

ASTM (Am. Soc. Testing and Materials), 1993, *Standards for refractories etc.: Vol. 15.01.*

Branigan, K., 1974, *Aegean metalwork of the Early and Middle Bronze Age*, Oxford Univ. Press, Oxford.

Bronitsky, G., 1986, The use of materials science techniques in the study of pottery construction and use, in *Advances in archaeological method and theory: Vol. 9* (ed. M. B. Schiffer), 209–76, Academic Press, Orlando.

Bronitsky, G., and Hamer, R., 1986, Experiments in ceramic technology: the effects of various tempering materials on impact and thermal-shock resistance, *Am. Antiquity*, **51** (1), 89–101.

Day, P. M., 1988, Ceramic analysis and pottery systems: the case of Minoan Crete, in *New aspects of archaeological science in Greece* (eds. R. E. Jones and H. W. Catling), 39–45, Fitch Lab. Occas. Pap., **3**, Athens.

Day, P. M., forthcoming, Marriage and mobility: traditions and the dynamics of the pottery system in twentieth-century east Crete, in *Pseira II* (eds. P. P. Betancourt and C. Davaras), Univ. Mus. Press, Philadelphia.

Dobres, M.-A., and Hoffman, C. R., 1994, Social agency and the dynamics of prehistoric technology, *J. Archaeol. Method Theory*, **1** (3), 211–58.

Feathers, J. K., 1989, Effects of temper on strength of ceramics: response to Bronitsky and Hamer, *Am. Antiquity*, **54** (3), 579–88.

Feathers, J. K., and Scott, W. D., 1989, Prehistoric ceramic composites from the Mississipi Valley, *Am. Ceram. Soc. Bull.*, **68**, 554–7.

Hertzberg, R. W., 1989, *Deformation and fracture mechanics of engineering materials*, John Wiley and Sons, Chichester.

Hoard, R. J., O'Brien, M. J., Khorasgany, M. G., and Gopalaratnam, V. S., 1995, A materials-science approach to understanding limestone-tempered pottery from the Midwestern United States, *J. Archaeol. Sci.*, **22**, 823–32.

Kilikoglou, V., Vekinis, G., and Maniatis, Y., 1995, Toughening of ceramic earthenwares by quartz inclusions: an ancient art revisited, *Acta Metallurgica et Materialia*, **43** (8), 2959–65.

Kolb, C. C., 1989, Ceramic ecology in retrospect: a critical review of methodology and results, in *Ceramic ecology in retrospect, 1988: current research on ceramic materials* (ed. C. C. Kolb), 261–375, Brit. Archaeol. Rep. Internat. ser., **513**, Oxford.

Lawn, B., 1993, *Fracture of brittle solids*, 2 edn., Cambridge Univ. Press, Cambridge.

Lemonnier, P. (ed.), 1993, *Technological choices: transformation in material cultures since the Neolithic*, Routledge, London.

MacKenzie, J. K., 1950, The elastic constants of a solid containing spherical holes, *Proc. Phys. Soc. (London) B*, **63**, 2–11.

Maniatis, Y., and Tite, M. S., 1981, Technological examination of Neolithic–Bronze Age pottery from central and south-east Europe and from the Near East, *J. Archaeol. Sci.*, **8**, 59–76.

Maniatis, Y., Whitebread, I., Jones, R. E., Simopoulos, A., Kostikas, A., and Williams, C. K., 1984, Punic amphoras found at Corinth, Greece: an investigation of their provenance and technology, *J. Field Archaeol.*, **11**, 205–22.

Marinatos, S., 1973, *Excavations at Thera: Vol. VII*, Athens.

Matson, F. R., 1965, *Ceramics and man*, Methuen, London.

Munz, D., Bubsey, R. T., and Shannon (Jun.), J. L., 1980, Fracture toughness determination of alumina using four-point-bend specimens with straight-through and chevron-notches, *J. Am. Ceram. Soc.*, **63**, 300–5.

O'Brien, J., Holland, T. D., Hoard, R. J., and Fox, G. L., 1994, Evolutionary implications of design and performance characteristics of prehistoric pottery, *J. Archaeol. Method Theory*, **1** (3), 259–304.

Rice, P., 1986, *Pottery analysis. A sourcebook*, Univ. Chicago Press, Chicago.

Rye, O., 1976, Keeping your temper under control: materials and manufacture of Papuan pottery, *Archaeol. Physical Anthropol. Oceania*, **11** (2), 106–37.

Shepard, A. O., 1965, *Ceramics for the archaeologist*, Carnegie Inst. Public., **609**, Washington, DC.

Skibo, J. M., 1992, *Pottery function: a use-alteration perspective*, Plenum Press, New York.

Srawley, J. E., 1976, Fracture toughness in plain strain, *Internat. J. Fracture Mech.*, **12**, 475–82.

Steponaitis, V., 1984, Technological studies of prehistoric pottery from Alabama: physical properties and vessel function, in *The many dimensions of pottery: ceramics in archaeology and anthropology* (eds. S. E. van der Leeuw and A. C. Pritchard), 79–127, Univ. Amsterdam, Amsterdam.

Tite, M. S., and Maniatis, Y., 1975, Scanning electron microscopy of fired calcareous clays, *Trans. Brit. Ceram. Soc.*, **74**, 19–22.

van der Leeuw, S. E. 1989, Risk, perception, innovation, in *What's new? A closer look at the process of innovation* (eds. S. E. van der Leeuw and R. Torrence), 300–29, Unwin Hyman, London.

Vekinis, G., and Kilikoglou, V., 1998, Mechanical performance of quartz-tempered ceramics: Part II, Hertzian point loading, wear resistance and application to ancient pottery, *Archaeometry*, **40** (2), 281–92.

Vekinis, G., Ashby, M. F., and Beaumont, P. W. R., 1990, R-curve behaviour of alumina ceramics, *Acta Metallurgica et Materialia*, **38**, 1151–62.

Vekinis, G., Ashby, M. F., and Beaumont, P. W. R., 1993, Plaster-of-Paris as a model material for brittle porous solids, *J. Materials Sci.*, **28**, 3221–7.

Wang, J. C., 1984, Young's modulus of porous materials: Part 1, Theoretical derivation of modulus-porosity correlation, *J. Materials Sci.*, **19**, 801–8.

Whitelaw, T. M., Day, P. M., Kiriatzi, E., Kilikoglou, V., and Wilson, D. E., 1997, Pottery traditions at Myrtos Fournou Korifi, Crete, in *TEXNH: craftsmen, craftswomen and craftsmanship in the Aegean Bronze Age* (eds. P. P. Betancourt and R. Laffineur), 265–74, Aegeaum vol., Liège.

Wright, R., 1986, The boundaries of technology and stylistic change, in *Ceramics and civilization: Vol. II* (ed. W. D. Kingery), 1–20, Am. Ceram. Soc., Columbus.

## APPENDIX: MECHANICAL PROPERTIES OF BRITTLE MATERIALS

*Fracture and fracture toughness*

There exists a critical stress under which a vessel containing cracks or flaws of given size would fail catastrophically. At this stress, the energy absorbed per unit area of crack $\alpha$ in order to advance is called toughness ($G_c$) (Ashby and Jones 1996).

$G_c$ is sometimes also called the 'critical strain energy release rate' and it provides an estimate of a material's resistance to crack propagation. It is a material property, which depends on the basic properties of the material and not on the size and concentration of the flaws or inclusions existing in the material (Lawn 1993). In the case of tempered ceramics $G_c$ is a property of the base clay.

In ceramics, failure occurs by fast fracture (unstable crack propagation) and, thus, $G_c$ is the energy expended in breaking atomic bonds per unit area and is given by:

$$G_c = \frac{\sigma^2 \pi \alpha}{E} \tag{4}$$

where $\sigma$ is the stress at failure (fracture strength) and $E$ is Young's modulus. The above equation gives the condition for the onset of fast fracture:

$$\sqrt{EG_c} = \sigma\sqrt{\pi\alpha} \tag{5}$$

and indicates that fracture will occur when a brittle material containing cracks of maximum size $\alpha$ is subjected to some critical stress $\sigma$. The right-hand side of the equation is the critical stress intensity factor or fracture toughness, $K_c$.

Therefore, fracture toughness is a property of the material and is routinely measured in engineering using notched specimens, thereby providing the necessary 'maximum size flaw' in order to apply equation (5). Of the three different displacement modes (tensile-I, shear-II, antiplane shear-III), mode I is encountered in the majority of engineering situations and, therefore, toughness and fracture toughness are usually related to it and expressed as $G_{Ic}$ and $K_{Ic}$ respectively (Hertzberg 1989). Materials with high total $K_{Ic}$ (and $G_{Ic}$) are less sensitive to flaws and other stress concentrators and, therefore, are more reliable for use.

In the case of brittle materials, $G_{Ic}$ can be considered as the intrinsic fracture energy of a material and, when failure occurs by fast, unstable crack propagation (curve (a) in Fig. 2), it expresses all the energy dissipated during fracture. In this case it is determined by measuring $K_{ic}$ and then applying equation (5). However, in composites of a brittle matrix with secondary phases (such as tempered ceramics), it is possible to obtain stable crack propagation (Fig. 2 (b)) after initial matrix fracture (due to the action of various toughening mechanisms) and, therefore, the calculated intrinsic toughness of the matrix $G_{Ic}$ is only part of the total energy dissipated. A significant portion of the total is the energy expended in propagating the stable crack until final failure, that is, the 'toughening component', denoted by $G_t$, and, on a load-displacement curve, it is displayed as the 'tail' of the curve after initial fracture, as shown by the shaded region in curve (b) of Figure 2. It can be estimated by measuring the area under the last part of the curve, by integration. Therefore, the total energy dissipated, $G$ in such systems, is $G_{ic} + G_t$ (Kilikoglou *et al.* 1995). To conclude, for unstable crack propagation $G = G_{ic}$ (as $G_t = 0$) and for stable crack propagation $G = G_{ic} + G_t$.

Knowledge of the total energy dissipated allows an estimation of the stability of a brittle vessel, for example, a pot. Pots with high $G$ will exhibit high resistance to crack propagation (thus avoiding fast catastrophic failure) and the stable, slow, development of macrocracks before final failure would offer enough warning to a user. It is, thus, clear that this kind of pottery offers improved reliability. Fractured pottery with high toughness may not collapse catastrophically, as any further crack propagation will require higher amounts of energy. Ancient potters and consumers may have been aware of this as large vessels have been found which have large cracks in their bodies but also bear traces of repair (Branigan 1974; Marinatos 1973).

*Fracture strength*

The fracture strength of a brittle material is the maximum stress at the point of failure during loading. It is usually measured by loading a beam in flexure and calculating the transverse rupture strength (TRS) (sometimes called the modulus of rupture) and it is usually larger than the actual tensile strength of a material by a factor of about 1.5 (Ashby 1992). Fracture strength is *not* a material property but depends greatly on the existence and size of any flaws and other stress concentrators in the specimen. It is, nevertheless, routinely used for strength assessment of brittle materials such as ceramics. Earthenware ceramics consist of many phases of variable crystallization and contain a large number of stress concentrating flaws and, therefore, the effect of flaw size on their strength can only be studied statistically. Using Weibull statistics (Ashby and Jones 1996) it is possible to determine the extent of strength variability and give a measure of reproducibility.

*Young's modulus*

The tensile stress $\sigma$ (tensile force $F$ divided by the cross-sectional area $A$) that a uniform rod is subjected to is related to the strain $\varepsilon$ (deformation divided by the initial length), by

$$\sigma = E\varepsilon \tag{6}$$

and Young's modulus $E$ is thus defined as 'the slope of the linear elastic part of the stress-strain curve' (Ashby 1992), a parameter which may be used to measure $E$ in practice. Ceramics, including pottery, have relatively high $E$ and, therefore, exhibit little deformation even at great stresses. Young's modulus, although a material property, is sensitive to the presence of pores, cracks and other imperfections in it (MacKenzie 1950). In the case of composites, $E$ can be calculated by a simple rule of mixtures, if the value of each of the components is known (Ashby 1993).